10-28-2017

Bubble-pump-driven LiBr-H2O and LiCl-H2O Absorption Air-Conditioning Systems

Julia Aman
University of Windsor

Paul Henshaw
University of Windsor

David S-K Ting
University of Windsor

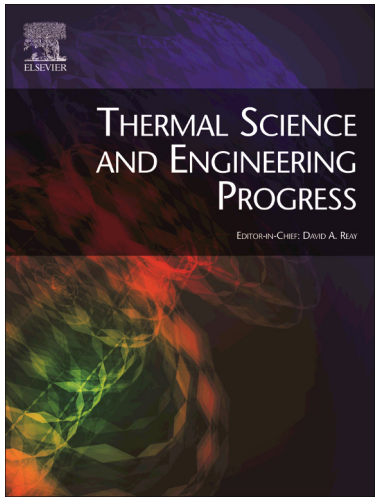

Bubble-pump-driven LiBr-H_2O and LiCl-H_2O Absorption Air-Conditioning Systems

Julia Aman, Paul Henshaw, David S-K Ting

PII: S2451-9049(17)30205-6
DOI: https://doi.org/10.1016/j.tsep.2017.10.022
Reference: TSEP 86

To appear in: *Thermal Science and Engineering Progress*

Received Date: 17 July 2017
Revised Date: 3 October 2017
Accepted Date: 28 October 2017

Please cite this article as: J. Aman, P. Henshaw, D. S-K Ting, Bubble-pump-driven LiBr-H_2O and LiCl-H_2O Absorption Air-Conditioning Systems, *Thermal Science and Engineering Progress* (2017), doi: https://doi.org/10.1016/j.tsep.2017.10.022

Bubble-pump-driven LiBr-H_2O and LiCl-H_2O Absorption Air-Conditioning Systems

Julia Aman[1], Paul Henshaw[2], David S-K Ting[3]
Turbulence and Energy Laboratory, Centre for Engineering Innovation, University of Windsor
401 Sunset Avenue, Windsor, ON, N9B 3P4, Canada

Abstract
A thermally-driven bubble pump, powered by solar or waste heat energy, is a simple and efficient technique for lifting a liquid from lower to higher levels, after which it can flow by gravity. In this study, solar thermal driven pumps were incorporated in the solar collector as well as in the refrigerant cycle to provide a design of an air-conditioning system for a residential home that is independent of grid electricity. The crystallization challenge, low pressure, and low efficiency are the main downsides of bubble-pump-driven LiBr-H_2O refrigeration systems, in comparison with other bubble-pump-driven diffusion absorption refrigeration systems. Therefore, a complete thermodynamic analysis of each component is necessary to improve the system performance. In this research, a thermodynamic model was developed, introducing a new absorbent-refrigerant pair (LiCl-H_2O) and comparing it with LiBr-H_2O, in a bubble pump operated absorption chiller driven by solar thermal energy. Under the same operating condition, the highest cooling effect and the performance of the LiCl-H_2O system are 49 W and COP=0.56 compared to 34 W and COP=0.46 for a LiBr-H_2O system.

Keywords: Bubble pump; vapor absorption refrigeration; energy analysis; LiBr-H_2O; LiCl-H_2O; COP

1. Introduction

Due to climate change, population growth, and increasing standard of living conditions, residential and small commercial air-conditioning demands are increasing significantly. Building heating and cooling systems account for 50% of the total global energy consumption [1]. In tropical countries, 70% of the total household energy is being used by air-conditioning systems [2]. The traditional vapor compression refrigeration systems usually used for providing cooling comfort cause a high-energy demand during the peak load period in the summer. Solar thermal powered air-condition systems are a sustainable way to provide the cooling comfort while reducing energy demand. The highest solar radiation also occurs during this peak period in summer. The abundance of solar energy in tropical and developing countries all year round can offer a suitable alternative in cooling technologies, particularly for off-grid communities. Thermally-driven absorption cooling systems can provide air-conditioning during the summer without compromising the grid electricity and their effect can be extended into the evening by storing solar thermal energy. Furthermore, since the phase out of CFCs (chlorofluorocarbons) and HCFCs (hydrochlorofluorocarbons) [3], the absorption refrigeration system, which uses an environmentally-friendly low global warming potential refrigerant, is a sustainable cooling technology for curbing greenhouse gas emissions.

[1] corresponding author, amanj@uwindsor.ca (J.Aman)
[2] henshaw@uwindsor.ca (P.Henshaw)
[3] dting@uwindsor.ca (D.Ting)

A vapor absorption refrigeration system (VARS) can be driven by waste heat or solar thermal energy. LiBr-H_2O and NH_3-H_2O are the most common refrigerant-absorbent working pairs for this VARS. The LiBr-H_2O absorption system has the advantage of higher efficiency, but due to its crystallization and corrosion problems, NH_3-H_2O is more preferable for small scale commercial or residential applications [4]. The core components of absorption cooling systems are the absorber, generator, condenser and evaporator. A pump is a critical component of the absorption system to circulate the refrigerant–absorbent solution from the low-pressure absorber to the high-pressure generator. High quality mechanical/electrical energy is used to run this pump. Furthermore, the pump must handle high temperature corrosive solutions. A thermally-driven bubble pump, which can be powered by waste heat or solar thermal energy, can be employed to circulate the liquid solution and generate the necessary refrigerant for the required cooling effects [5]. In the diffusion-absorption refrigeration cycle, a bubble pump or vapor-lift pump can be used to circulate the solution from the generator to the absorber without electrical work input. In a bubble pump, the vapor created (via heating) increases the buoyancy of the fluid, causing it to ascend through a vertical tube under two-phase flow conditions. For small scale applications like residential air-conditioning, this system will be more reliable and independent of the availability of electricity. But for larger scale applications of a bubble-pump-operated VARS, multiple parallel pumps may be explored [6].

The conventional absorption refrigeration cycle works at two pressure levels to achieve the saturation temperature difference between the condenser and the evaporator. But in a diffusion absorption refrigeration system, the circulation of the solution is carried out by the bubble pump, maintaining essentially a single pressure throughout the entire cycle. This was first introduced by Platen and Munters in 1920 [7]. Although it is called a ‘single pressure’ system, there are still minor pressure variations due to the flow friction and gravity. A heat-driven bubble pump is a mechanism to move the fluid through the cycle against this flow friction and gravity. As a result, this thermally-driven absorption cycle does not require any electricity to create the pressure difference. Bubble pumps are portable, operate silently, have high reliability and are inexpensive to build [8]. These advantages make this system ideal for remote locations and to where electricity is not available. However, their widespread application is somewhat hindered because of their low COP compared to a conventional absorption system.

The single pressure absorption system cycle works on two thermodynamic cycles: the ammonia-water-hydrogen cycle and the Einstein cycle. The most familiar is the ammonia-water-hydrogen cycle which is known as the diffusion absorption refrigeration (DAR) cycle patented by Swedish engineers Platen and Munter in1920 [7]. This cycle uses at least three working fluids to achieve a low evaporation temperature and high condensation temperature at a single pressure level. The third, an inert fluid is introduced to the working fluid to lower the partial pressure of the refrigerant in the evaporator and maintaining pressure equalization throughout the system. Thus the refrigerant can evaporate at a lower temperature in the evaporator. The most common working fluids for this cycle are ammonia-water-hydrogen/helium where ammonia is the refrigerant, water is the absorbent and hydrogen or helium is the inert gas which provides the pressure equalization of the system. In the Platen and Munter cycle, the refrigerant ammonia is absorbed by the water and its partial pressure is lowered by the inert gas hydrogen or helium. The water separates the ammonia from the inert gas. In 1930, Albert Einstein and Szilard Leo disclosed another single pressure refrigeration cycle which uses butane, ammonia, and water [9]. Unlike the Platen and Munter cycle, the Einstein cycle utilizes absorbate fluid for pressure equalization instead of an inert gas. In this cycle, butane works as the refrigerant, ammonia is

used to lower the partial pressure of the refrigerant, and water is used to absorb the ammonia and separate the butane. The Platen and Munter refrigeration cycle has been used for refrigerators in homes, RV's and hotel rooms since the 1920's. The COP of this cycle is 0.15 to 0.2 [8]. Because of the lower efficiency of this cycle compared to a conventional absorption cycle, research has been conducted to improve the efficiency, and with the variation of the evaporator temperature, the best published COP is approximately 0.3 [10, 11]. Though the Einstein cycle was patented in 1930, the first detailed study of the cycle was by George Alefeld in 1980. With many simplifying assumptions, he found the cycle COP to be 0.25 [12]. In 1997, Delano analyzed this cycle performance in detail based on Stenning and Martin's analysis and improved the cycle performance by adding two regenerative heat exchangers in this cycle. The best COP was 0.4 [9].

Water-based refrigerant VARSs like LiBr-H_2O work on low (vacuum) pressure, whereas NH_3-H_2O is a high-pressure refrigeration system. As a result, when a bubble pump is used for a water-based refrigerant VARS, the refrigeration cycle does not work as in DAR systems. Pfaff et al. [13] were the first to study the bubble pump for use in a LiBr-H_2O refrigeration system and the bubble pump was modelled based on intermittent slug flow using the manometer principal. The performance of the bubble pump was evaluated experimentally in a glass tube test rig to visualize the flow behavior. Saravanan and Maiya [6] designed and built a 50 W bubble pump operated LiBr-H_2O VARS and tested it with different operation conditions [6]. In their design, they restricted the refrigerator height to 1.5 m to operate the system with a low-pressure difference between the condenser and the evaporator. They used a parallel flow path and a combination of 'U' tube and capillary tubes to reduce the pressure drop between the condenser and the evaporator.

The pressure difference between the evaporator and the condenser should be low to operate the bubble pump in water-based refrigeration systems [6]. The water vapor pressure difference between the condenser and the evaporator of a water-salt refrigeration system is low enough to employ the bubble pump to circulate the solution and refrigerant in the system. The pressure drop in the connecting tubes and in the system components is a major concern for this system because it operates under a vacuumed pressure. For a conventional LiBr-H_2O VARS, equal-pressure components are used to minimize the pressure loss, but the pressure drop could be high in small scale applications [6]. Hence, little research has been carried out to use bubble pumps in LiBr-H_2O VARS and commercial applications are not yet practicable.

The performance of VARSs strongly depends on the thermophysical properties of the refrigerant-absorbent working fluids [14]. Saravanan and Maiya studied water based refrigerant working fluids for VARSs and found that LiCl-H_2O has advantages over LiBr-H_2O in terms of the system performance as well as for low energy consumption. They suggested that the lower circulation ratio (ratio of the mass flow rate of salt solution and refrigerant) in LiCl-H_2O systems is the cause of higher performance [15]. Grover et al. [16] analyzed the thermodynamic properties of LiCl-H_2O for VARSs and found that this solution can operate at lower generator temperature. A thermophysical properties analysis of different working fluids for VARSs was performed by Flores et al. [17] and it was found that LiCl-H_2O has a higher COP over a LiBr-H_2O VARS at lower heat input because of their low C_p (heat capacity) values. Gogoi and Konwar [18] performed exergy analysis of LiCl-H_2O VARSs and observed that at the same operating conditions, LiCl-H_2O systems had higher COP and exergetic efficiency values than LiBr-H_2O systems. They suggested that the thermodynamic properties of LiCl-H_2O solution account for this higher efficiency. Recently, She et al. [19] proposed a low-grade heat-driven

double-effect VARS where LiCl-H_2O was used on the high-pressure side and LiBr-H_2O was utilized on the low-pressure side because LiCl-H_2O has a larger vapor pressure that LiBr-H_2O. Bellos et al. [22] investigated the LiCl-H_2O working pair for a double-effect absorption chiller driven by a solar thermal collector and found that it can achieve 8% more cooling compared to a LiBr-H_2O system.

Since low efficiency is the main downside of bubble-pump-operated absorption refrigeration systems, a complete thermodynamic analysis of each component is necessary. As the cycle efficiency depends on the amount of refrigerant desorbed from the generator, so the detailed analysis of the bubble pump generator is needed before one can improve the system efficiency. Since water is the better refrigerant for VARS, especially for air-conditioning applications, and also because of the limitation of LiBr-H_2O use in bubble-pump-operated absorption systems due to its low vapor pressure, the present research has incorporated the thermophysical properties of LiBr-H_2O and LiCl-H_2O in the bubble pump modelling. This study has also focused on the development of a mathematical simulation model for the bubble pump generator by using a two-phase flow model that will determine the cooling effect of the refrigeration cycle and a thermodynamic model of every component of this cycle in order to achieve the maximum system efficiency.

2. System Description

A schematic of a bubble-pump-operated water-based refrigerant vapor absorption refrigeration system which can be driven by solar thermal energy is shown in Figure 1. In order to make the system completely independent of the grid electricity, the solar collector is also operated by a solar bubble pump in this figure. The air-cooler with the solar collector is used only for cooling the vapor that may be produced from the collector. For the thermodynamic performance analysis of the absorption air-conditioning system, only the refrigeration cycle (absorption air-conditioning cycle in Figure 1) operation is described and analyzed in this study. In an absorption air-conditioning system, the pure water vapor flows to the condenser (State 1) from the separator, and is condensed by releasing '$\dot{Q}_{cond}$' heat to the atmosphere by air cooling. Then the condensed, saturated water (State 2) flows to the evaporator through the throttle valve where its pressure is reduced for the necessary cooling effect ($\dot{Q}_{eva}$) in the evaporator (State 3). The water vapor from the evaporator (State 4) is absorbed in the absorber by the high-concentration (strong) salt solution, which comes back from the bubble pump generator, and becomes a low-concentration (weak) salt solution. The weak solution from the absorber (State 5) flows to the bubble pump generator through the heat exchanger (State 6) by gravity. In the bubble pump generator, the solution is heated by solar heat input ($\dot{Q}_{bubble\ pump}$). When the temperature of water in the solution is higher than the saturation temperature, bubbles of water vapor start to form. Many small vapor bubbles coalesce into a big bubble and rise in the bubble pump tube, carrying the solution above it into the separator. Water vapor separates from the solution in the separator and the solution becomes strong (State 7) and drains back to the absorber through the solution heat exchanger. The strong solution in the absorber rejects heat ($\dot{Q}_{abs}$) to the atmosphere and absorbs the water vapor from the evaporator.

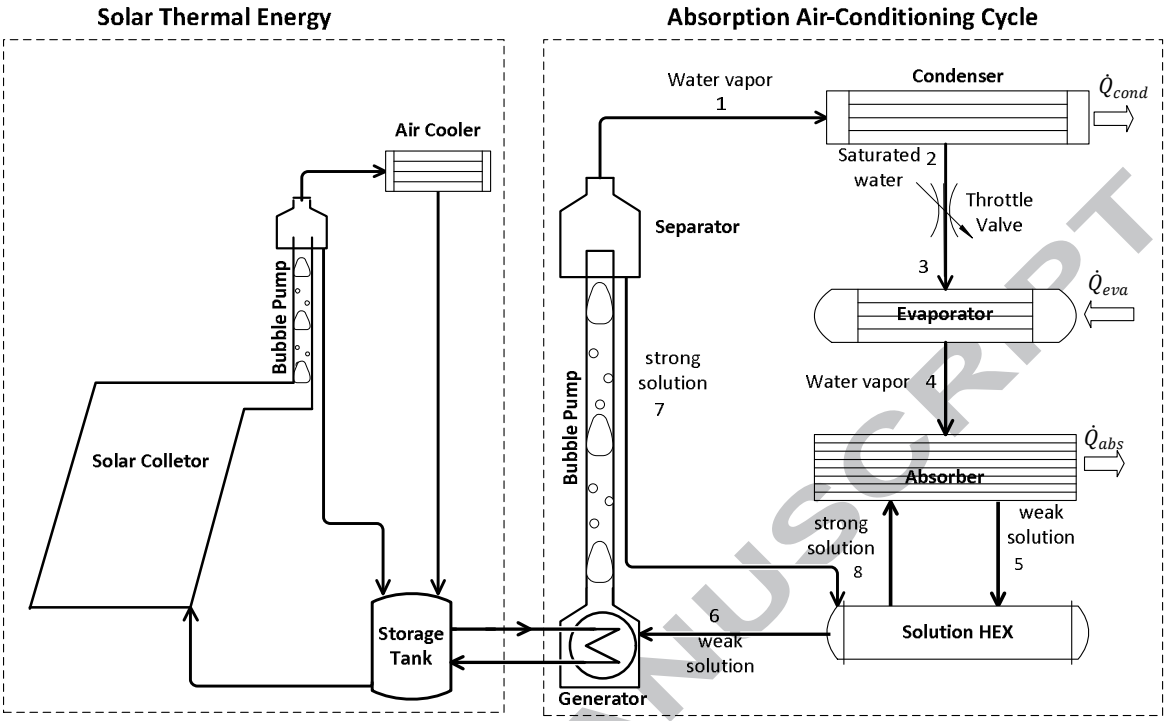

Figure 1: Flow diagram of solar absorption air-conditioning system

3. Thermodynamic and Simulation Model

For a thermodynamic model of the bubble pump operated refrigeration cycle, the principles of mass and energy conservation have been applied for each component of the system. In this study, the main components: generator and bubble pump, condenser, evaporator, gas heat exchanger, absorber, and solution heat exchanger have been studied. To analyze the thermodynamic cycle, a control volume is applied to each component.

Generator and the bubble pump:

The bubble pump heat input to the generator evaporates the water vapor and separates it from the solution as shown in Figure 2. The strong solution is pumped back to the solution heat exchanger through the bubble pump and separator. The mass and energy balance of the generator and the bubble pump control volume yields:

$$\dot{m}_6 = \dot{m}_1 + \dot{m}_7 \quad (1)$$

Energy balance: $$\dot{Q}_{gen} = \dot{m}_1 h_1 + \dot{m}_7 h_7 - \dot{m}_6 h_6 \quad (2)$$

The species conservation equation for salt solution in the generator is:

$$X_6 \dot{m}_6 = X_7 \dot{m}_7 \quad (3)$$

where X is the LiBr or LiCl mass fraction in solution.

Bubble pump modeling:

The mass flow rate of refrigerant strongly depends on the bubble pump parameters (such as lift tube diameter (D), lift tube length (L), height (H) of the liquid in the lift tube) and the heat input to the bubble pump ($\dot{Q}_{bubble\ pump}$). The bubble pump consists of a lift tube connecting the generator and separator. The generated vapor bubbles rise in the tube lifting the solution ahead of it into the separator.

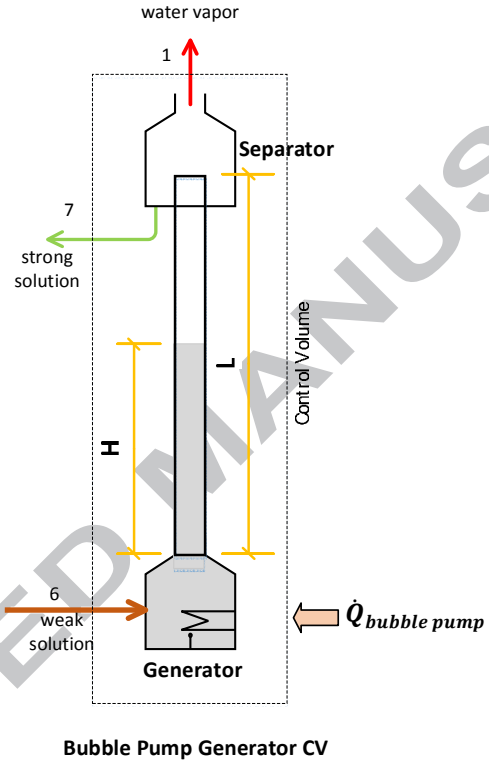

Figure 2: Bubble Pump Generator Control Volume

In this analysis, a two-phase flow model is used to determine the flow rate of the weak solution in the bubble pump. The following analytical model, taken from Aman et al. has been used to describe the bubble pump performance [5].

The void fraction is the ratio of volume of the gas in the liquid over total volume of the liquid gas mixture, an important parameter in two-phase flow to determine the flow regime as well as two-phase pressure drop and heat transfer [5]. It can be determined as

$$\propto_d = \frac{volume\ of\ the\ gas\ in\ the\ liquid}{total\ volume\ of\ the\ liquid\ gas\ mixture} = \frac{\dot{V}_g'}{C_o\left(\dot{V}_l' + \dot{V}_g'\right) + v_b'} \quad (4)$$

where,

$$\dot{V}_l' = \frac{\dot{V}_l}{A(gD)^{1/2}}, \qquad \dot{V}_g' = \frac{\dot{V}_g}{A(gD)^{1/2}}, \qquad v_b' = \frac{v_b}{(gD)^{1/2}} \tag{5}$$

C_o is the velocity profile coefficient of gas-liquid mixture (ranging from 1.2 for fully-developed turbulent flow to 2 for laminar flow [20]), v_b' is the non-dimensional vapor bubble velocity, v_b is the velocity of a vapor bubble in stagnant liquid (m/s), $\dot{V}_l'$ is the non-dimensional volume flow rate of liquid, $\dot{V}_l$ is the volumetric flow rate of liquid (m^3/s), $\dot{V}_g'$ is the non-dimensional volume flow rate of vapor, $\dot{V}_g$ is the volumetric flow rate of gas (m^3/s), A is the cross sectional area of the lift tube (m^2), and D is the inner diameter of the lift tube.

From theoretical and experimental analysis, Reinemann [20] showed that non-dimensional vapor bubble velocity can be expressed as the surface tension parameter:

$$V_b' = 0.352(1 - 3.18\Sigma - 14.77\Sigma^2) \tag{6}$$

where,

$$\text{surface tension parameter}, \Sigma = \frac{\sigma}{\rho g D^2} \tag{7}$$

If the lift tube length is L and it is partially filled with the liquid solution with height H, which is the height of the absorber, the total pressure drop along the lift tube is the sum of the static pressure drop and the frictional losses, and can be calculated by [5]

$$\rho g H = \rho g((1 - \propto_d)L + f\frac{L}{2D}\rho v_m^2\,(1 - \propto_d) \tag{8}$$

where, f is the friction factor for continuous flow [22] given by

$$f = \frac{0.316}{Re^{0.25}} \tag{9}$$

Re is the Reynolds number for a solution in liquid and vapor phase and expressed as

$$Re = \frac{\rho_{sol} v_m D}{\mu} \tag{10}$$

The following equation can be established by rearranging Equation (8),

$$\frac{H}{L} = (1 - \propto_d)\left(1 + \frac{f}{2}\left(\dot{V}_l' + \dot{V}_g'\right)^2\right) \tag{11}$$

The flow rate of vapor depends on the heat addition to the generator which is the required heat for the bubble pump. Assuming that there is no heat loss through the lift tube of the bubble pump and the generator, the required heat input will be used to determine the volumetric flow rate of vapor by the following equation

$$\dot{Q}_{bubble\ pump} = \dot{V}_g \rho_g h_{fg} \tag{12}$$

And the mass flow rate of vapor refrigerant by the bubble pump is calculated by

$$\dot{m}_1 = \dot{V}_g \rho_g \tag{13}$$

The volume flow rate of the strong solution will be determined by using Equations 11 and 12. And the mass flow rate of the strong solution is

$$\dot{m}_7 = \dot{V}_l \rho_{sol} \tag{14}$$

To quantify the bubble pump generator performance, the lifting ratio is an important parameter that is determined by the volumetric flow rate of strong solution per volumetric flow rate of vapor and can be expressed as

$$b = \frac{\dot{V}_l}{\dot{V}_g} = \frac{\dot{m}_7}{\dot{m}_1} \tag{15}$$

Solution Heat Exchanger (SHX):

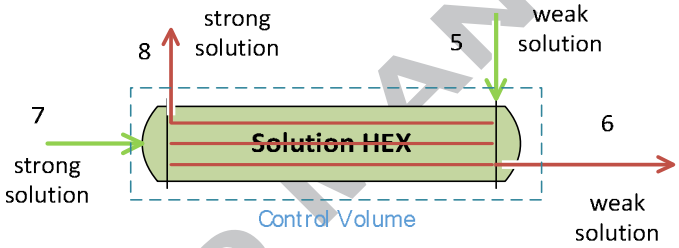

Figure 3: Solution Heat Exchanger Control Volume

Equations 16 and 17 represent the energy balance for the solution heat exchanger [4].

$$T_6 = \frac{\dot{m}_7}{\dot{m}_5}\eta_{HEX} T_7 + \left(1 - \frac{\dot{m}_7}{\dot{m}_5}\eta_{HEX}\right) T_5 \tag{16}$$

where η_{HEX} is the heat exchanger efficiency.

$$h_8 = h_7 - \frac{\dot{m}_5}{\dot{m}_7}(h_6 - h_5) \tag{17}$$

Absorber:

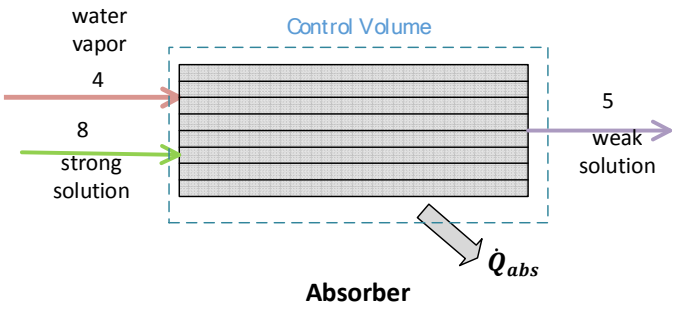

Figure 4: Absorber Control Volume

Energy balance of the absorber: $\dot{Q}_{abs} = \dot{m}_8 h_8 + \dot{m}_4 h_4 - \dot{m}_5 h_5$ (18)

Evaporator:

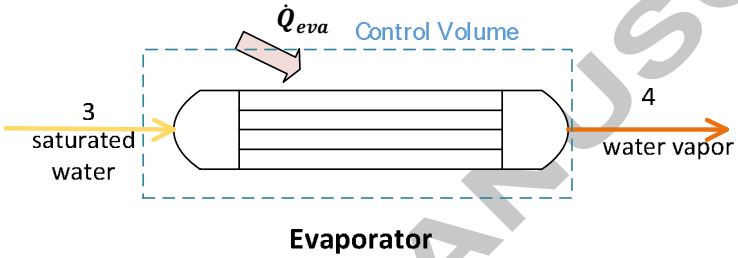

Figure 5: Evaporator Control Volume

Energy balance of the evaporator: $\dot{Q}_{eva} = \dot{m}_4 h_4 - \dot{m}_3 h_3$ (19)

Condenser:

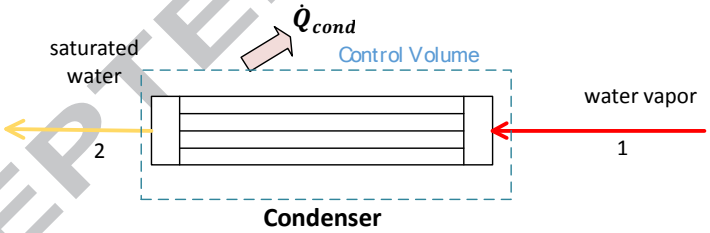

Figure 6: Condenser Control Volume

Energy balance of the condenser: $\dot{Q}_{con} = \dot{m}_1(h_1 - h_2)$ (20)

Cycle performance:

In a bubble pump operated VARS, the bubble pump solar heat input is the only primary energy input to the generator. The coefficient of performance of this system is defined as:

$$COP = \frac{useful\ energy\ output}{primary\ energy\ input} = \frac{\dot{Q}_{eva}}{\dot{Q}_{bubble\ pump}}$$

4. Thermodynamic properties

For the absorption air-conditioning cycle analysis, the thermodynamic properties and the concentration of the salt (LiBr/LiCl) in water are determined by using the Engineering Equation Solver (EES) software [21] at the equilibrium pressure and temperature for each state. The analysis is performed considering the fluid flow is steady and the system is in a steady-state condition.

5. Results and Analysis

The performance of each component of the bubble pump operated VARS has been predicted by the thermodynamic analysis and the bubble pump performance has been analyzed under two-phase fluid flow conditions. The coefficient of performance (COP) of the air-conditioning cycle has been calculated by using two working fluids (LiBr-H_2O and LiCl-H_2O).

In order to validate the proposed thermodynamic model in this study, the analysis of a LiBr-H_2O absorption system was compared with the experimental results of Saravanan & Maiya [6] in Figure 7. Saravanan & Maiya [5] reported that the temperature of generator fluctuated, which would result in lower performance of the system, compared to this steady-state analytical model. The COP was calculated at different generator heat inputs for 50 W of cooling capacity at the evaporator temperature of 7°C. It was clearly shown that the agreement between the analytical and the experimental results are very good; the average variation is within 3.2%.

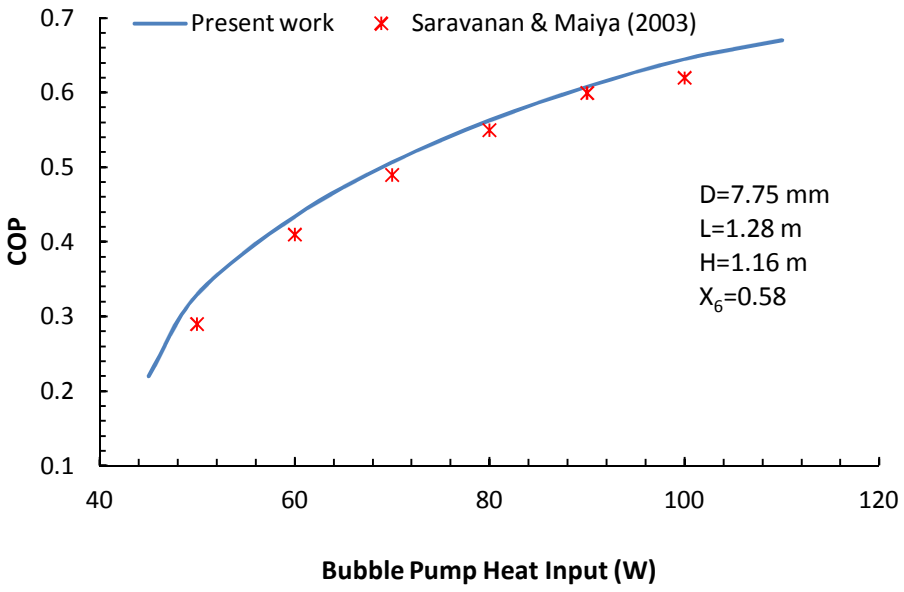

Figure 7: Performance comparison of a bubble pump operated LiBr-H_2O VARS between the proposed model and the experimental results of Saravanan & Maiya [6].

Various thermodynamic properties at different stages in the cycle operation of LiBr-H_2O and LiCl-H_2O absorption air-conditioning systems driven by bubble pump are shown in Table 1. The properties have been obtained from the cycle analysis at the operating condition of $T_{BP\,gen}$ =

70°C, T_{cond} = 35°C, T_{abs} = 35°C, T_{eva} = 7°C, the heat exchanger efficiency = 80%, and the bubble pump parameters: D=10 m, L= 0.47 m and H= 0.28 m. The results of the thermodynamic model analysis of two systems are presented in Table 2 which illustrates the strong and weak solution concentrations, system pressures and various energy flows to and from the systems. The lifting ratio and the cycle performance is also listed in the table.

Table 1: Thermodynamic properties at different states in LiBr-H_2O and LiCl-H_2O absorption cycles at operating conditions T_{gen} = 70°C, T_{cond} = 35°C, T_{abs} = 35°C, T_{eva} = 7°C, η_{HEX} = 80, D=10 mm, H=0.28 m, and L=0.47 m.

State	Temperature (°C)	Pressure (kPa)	Mass flow (g/s)		% Concentration		Enthalpy (kJ/kg)	
			LiBr-H_2O	LiCl-H_2O	LiBr-H_2O	LiCl-H_2O	LiBr-H_2O	LiCl-H_2O
Bubble pump generator ref exit (1)	70	5.627	0.014	0.021	100	100	2630	2630
Condenser ref exit (2)	35	5.627	0.014	0.021	100	100	147	147
Evaporator ref inlet (3)	7	1.002	0.014	0.021	100	100	147	147
Evaporator ref exit (4)	7	1.002	0.014	0.021	100	100	2513	2513
Absorber sol exit (5)	35	1.002	0.672	0.413	54.08	41.07	81	155
Sol HEX exit (6)	63	1.002	0.672	0.413	54.08	41.07	139	229
Sol HEX inlet (7)	70	1.002	0.518	0.335	55.60	43.77	157	265
Absorber sol inlet (8)	44	1.002	0.518	0.335	55.60	43.77	113	186

ref = refrigerant;
sol = solution

Table 2: Thermodynamic analysis of bubble pump operated LiBr-H_2O and LiCl-H_2O absorption air-conditioning systems

	LiBr-H_2O	LiCl-H_2O
Generator Temp (°C)	70	70
Mass fract. weak sol (X_6)	54.08%	41.07%
Mass fract. strong sol (X_7)	55.6%	43.77%
Vapor Pressure (kPa)	6.5	6.8
Bubble pump, $\dot{Q}_{bubble\ pump}$	73 W	87 W
Generator, $\dot{Q}_{gen}$	73 W	87 W
Evaporator, $\dot{Q}_{eva}$	34 W	49 W
Absorber, $\dot{Q}_{abs}$	70 W	78 W
Condenser, $\dot{Q}_{cons}$	37 W	58 W
COP	0.46	0.56
Lifting ratio, b	58.85	31.48

For the steady-state operation of a bubble-pump-driven VARS, the strong solution flow rate is determined based on the solution flow rate required to absorb the refrigerant vapor generated by the bubble pump. Therefore, the highest liquid (strong solution) flow rate by the pump is not desired as proportionally less vapor (refrigerant) is generated at this stage. Figure 8 shows that the lifting ratio increases sharply as the bubble pump heat input decreases. The lower

(lifting ratio) limit of these curves was determined by the conditions in Table 2. Lower heat inputs give excess liquid flow (strong solution), compared to vapor (refrigerant) flow. This is reflected in Figure 9. It shows that the strong solution mass flow is low at low heat input whereas the refrigerant flow rate is very low. Under these conditions, the refrigeration cycle cannot operate efficiently. As the heat input increases, the strong solution flow rate increases and after reaching a maximum it decreases sharply; whereas the refrigerant flow rate increases steadily as heat input increases. Therefore, it is impractical for this refrigeration cycle to operate at low heat input at these operating conditions. Comparing the LiBr-H_2O system and the LiCl-H_2O system, it is shown that the LiCl-H_2O can operate at higher heat input values. This results in higher vapor (refrigerant) generation which effects the system performance. According to the p-T-X (pressure, temperature and concentration) relationship, the salt concentration in the LiBr-H_2O system needs to be higher to acquire the required system pressure to operate the system. The minimum required pressure can be achieved for this system at the temperature of 70°C. At the operating condition described in Table 1, the minimum concentration of LiBr-H_2O in solution is 54%. The corresponding strong solution concentration is 56%. At a constant heat input, the required concentration becomes stronger/higher as the temperature increases, which would result in crystallization in the bubble pump generator as well as in the absorber. In contrast, but with the same operating conditions as the LiBr-H_2O system, the LiCl-H_2O requires a lower concentration of salt (41%) in the absorber and this system can operate up to a concentration of 51% before crystallization occurs. Hence, the LiCl-H_2O system can operate from 70 to 75°C, although there is little change in the COP (0.459 to 0.460) over this temperature range. As a result of the higher system pressure in the LiCl-H_2O system, a higher amount of refrigerant vapor will be produced as the heat input increases, resulting in a higher COP.

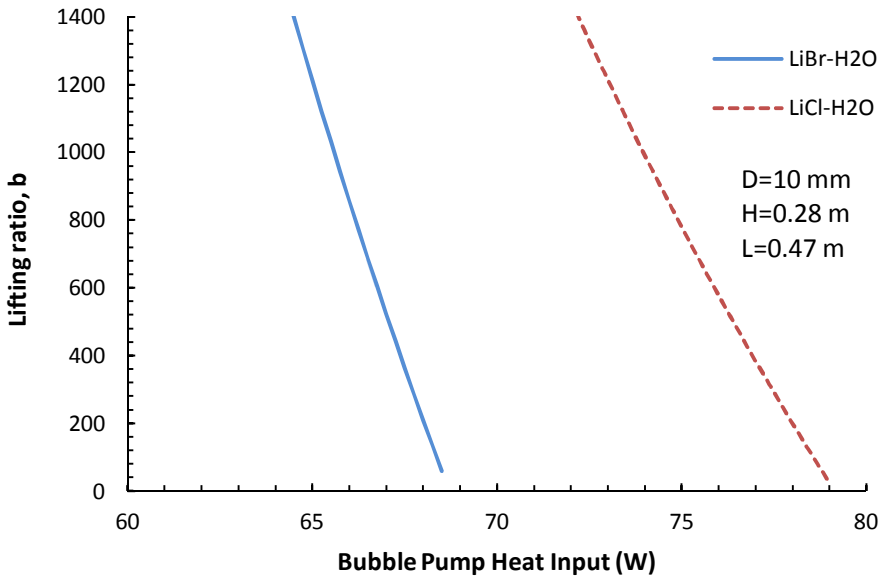

Figure 8: Lifting ratio of LiBr-H_2O and LiCl-H_2O VARS at different bubble pump heat input at T_{gen} = 70°C.

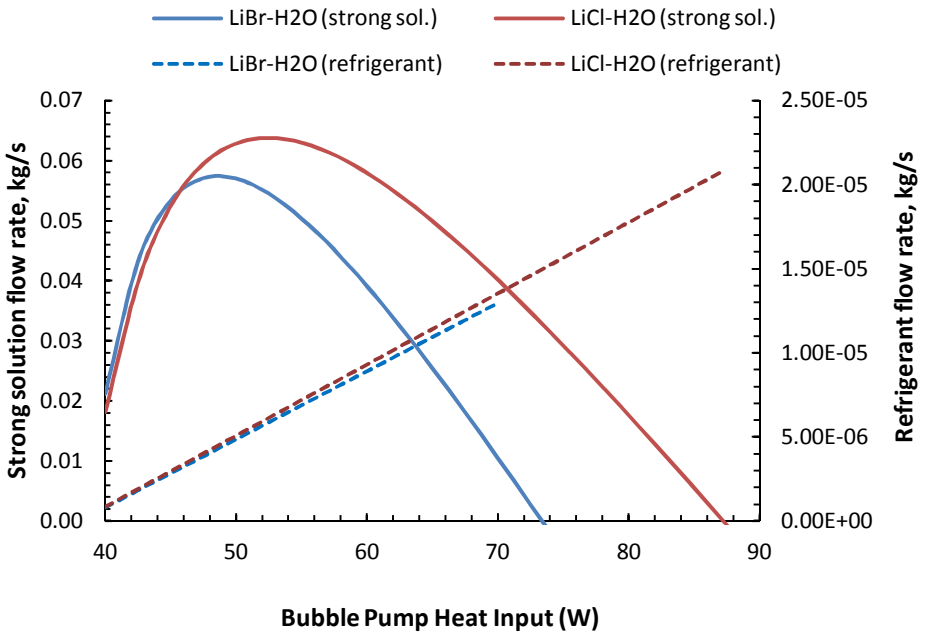

Figure 9: Strong solution and refrigerant flow rate by the bubble pump at different heat input at T_{gen} = 70°C for LiBr-H_2O and LiCl-H_2O.

The coefficient of performance of LiBr-H_2O and LiCl-H_2O systems is compared at different bubble pump heat inputs in Figure 10. The COP increases for both systems with increasing heat input but suddenly drops down at certain heat input. This is because the refrigerant vapor generation increases in the bubble pump generator as the heat input increases and this causes the lifting of liquid solution (strong solution) by the pump. The increasing vapor flow increases the gas void fraction in the two-phase flow mixture of the bubble pump lift tube. When the gas void fraction exceeds 80%, there is a liquid film around the tube wall and the core of the tube fills with vapor [9]. This is called churn flow, and as a result, there is no more liquid flow. This situation is reached at heat inputs of 73.2 W and 87.3 W for LiBr-H_2O and LiCl-H_2O systems, respectively, at the operating conditions mentioned in Table 1. This negative effect of increasing heat input causes the COP to drop down at a certain heat input and allows for the prediction of the highest COP of the system. In Figure 10, it is clearly seen that the COP is higher in a LiCl-H_2O system and it provides its highest performance at higher heat input compared to a LiBr-H_2O system. The highest performances for LiBr-H_2O and LiCl-H_2O systems were 0.46 at 73.2 W and 0.56 at 84.7 W, respectively.

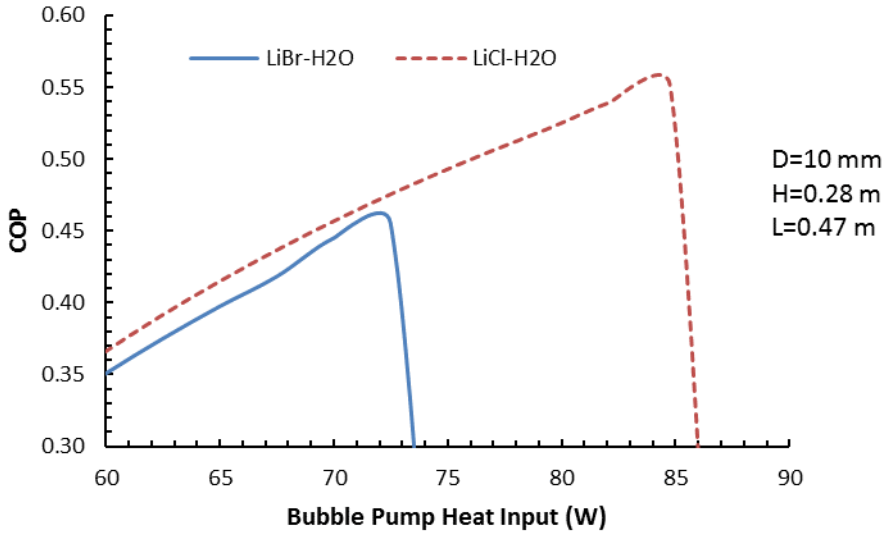

Figure 10: Coefficient of performance of LiBr-H_2O and LiCl-H_2O VARS at different bubble pump heat input at T_{gen} = 70°C, T_{cond} = 35°C, T_{abs} = 35°C, T_{eva} = 7°C, η_{HEX} = 80.

6. Conclusions

A water-based refrigerant vapor absorption refrigeration system (VARS), that can operate by a solar thermally-driven bubble pump, was analyzed in this study. In this refrigeration cycle, the pump is the key component for driving an air-conditioning system by generating the refrigerant vapor, as well as by pumping the liquid solution to absorb this refrigerant in the absorber. Therefore, the physical properties of the bubble pump were incorporated in this refrigeration cycle in order to analyze the whole cycle performance. A component-by-component thermodynamic model was developed to analyze the energy performance of the system, which lead to improving the system efficiency. The analysis was performed using two different working fluids in the bubble-pump-driven VARS. The LiCl-H_2O system operates at high efficiency due to its higher system pressure and thermophysical properties compared to the low pressure LiBr-H_2O system. The crystallization problem constrains the LiBr-H_2O system to operate at lower heat input with lower performance.

Overall, the model in this study will provide an effective tool to analyse water-based refrigerant VARS systems that can be driven by a bubble pump with solar heat input, and simulate the effect of bubble pump operation on steady-state system performance.

Acknowledgements

This work is made possible by the Natural Science and Engineering Research Council of Canada.

Nomenclature

A	area (m^2)
b	lifting ratio
COP	coefficient of performance
D	lift tube diameter (m)
g	acceleration due to gravity (m/s^2)
h	specific enthalpy (kJ/kg)
HEX	heat exchanger
H_2O	water
LiBr	lithium-bromide
LiCl	lithiu-cloride
$\dot{m}$	mass flow rate (kg/s)
P	pressure (kPa)
$\dot{Q}$	heat transfer rate (Watts)
ref	refrigerant
sol	solution
T	temperature (^oC)
X	mass fraction of salt in the solution
η_{HEX}	heat exchanger efficiency

Subscripts

abs	absorber
b	vapor bubble
cond	condenser
eva	evaporator
g	gas
gen	generator
l	liquid
sol	solution

References

[1] Kharseh M., Altorkmany L., Nordell B., Global warming's impact on the performance of GSHP, Renewable Energy, 36 (2011) 1485–1491.
[2] Prasartkaew B., Kumar S., Experimental study on the performance of a solar-biomass hybrid air-conditioning system, Renewable Energy 57 (2013) 86-93.
[3] United Nations Framework Convention on Climate Change (UNFCCC): Handbook. Bonn, Germany: Produced by Climate Change Secretariat, Intergovernmental and Legal Affairs, 2006 UNFCCC.
[4] Aman J, Ting DS-K, Henshaw P. 2014. Residential solar air conditioning: energy and exergy analyses of an ammonia-water absorption cooling system. Applied Thermal Engineering 62, 424-432.

[5] Aman, J., Henshaw, P. Ting, D. S-K., 2016, Modelling and Analysis of Bubble Pump Parameters for Vapor Absorption Refrigeration Systems, proceedings of ASHRAE Annual Conference, St. Louis, MO, USA, June 25 to 29.
[6] Saravanan R., Maiya MP., Experimental analysis of a bubble pump operated H_2O–LiBr vapor absorption cooler. Applied Thermal Engineering 23 (2003) 2383–2397.
[7] Platen, B.C. Munters, C.G., 1928. Refrigerator. U.S. Patent 1,685,764.
[8] White, S.J. Bubble Pump Design and Performance. MSc Thesis. Georgia Institute of Technology, Atlanta, USA. Mechanical Engineering. 2001.
[9] Delano A. Design Analysis of the Einstein Refrigeration Cycle, Ph.D. Thesis, Georgia Institute of Technology,1998, http://www.me.gatech.edu/energy/andy_phd.
[10] Jakob U, Eicker U, Schneider D, Taki AH, Cook MJ. Simulation and experimental investigation into diffusion absorption cooling machines for air conditioning applications. Applied Thermal Engineering 28(2008) 1138-1150.
[11] Starace G., Pascalis LD., 2012. An advanced analytical model of the diffusion absorption refrigerator cycle. International Journal of Refrigeration. 35, 605-612.
[12] Shelton S., Delano A., Schaefer L., Second Law Study of the Einstein Refrigeration Cycle, Proceedings of the Renewable and Advanced Energy Systems for the 21st Century, April 1999.
[13] Pfaff M., Saravanan R., Maiya MP, Srinivasa M. 1998. Studies on bubble pump for a water–lithium bromide vapor absorption refrigeration. International Journal of Refrigeration 21 (1998) 452–462.
[14] Perez BH., Absorption heat pump performance for different types of solution. Int. J. Refrigeration 7 (1984) 115-122.
[15] Saravanan R., Maiya MP., Thermodynamic comparison of water-based working fluid combinations for a vapour absorption refrigeration system, Applied Thermal Engineering 18(7) (1998) 553-568.
[16] Grover GS, Eisa MAR, Holland FA. Thermodynamic design data for absorption heat pump systems operating on water-Lithium Chloride–Part one. Cooling. Heat Recovery Syst CHP 8 (1988) 33-41.
[17] Flores V H F, Román JC, Alpírez GM, Performance analysis of different working fluids for an absorption refrigeration cycle, American Journal of Environmental Engineering 4(4A) (2014) 1-10, DOI: 10.5923/s.ajee.201401.01.
[18] Gogoi TK., Konwar D., Exergy analysis of a H_2O–LiCl absorption refrigeration system with operating temperatures estimated through inverse analysis, Energy Conversion and Management 110 (2016) 436–447.
[19] She X., Yin Y., Mengfei Xu M., Zhang, X., A novel low-grade heat-driven absorption refrigeration system with LiCleH2O and LiBreH2O working pairs, International Journal of Refrigeration 58 (2015) 219-234.
[20] Reinemann, D.J., Parlange, J.Y., Timmons, M.B., 1990. Theory of small-diameter airlift pump. Int. J. Multiphase Flow. 16, 113-122.
[21] EES (Engineering Equation Solver), 2015. F-Chart software, Academic Commercial V9. 941(1992-2015), www.fchart.com
[22] Bellos E., Tzivanidis C., Pavlovic S., Stefanovic V., Thermodynamic investigation of LiCl-H_2O working pair in a double effect absorption chiller driven by parabolic trough collectors. Thermal Science and Engineering Progress 3 (2017) 75–87.

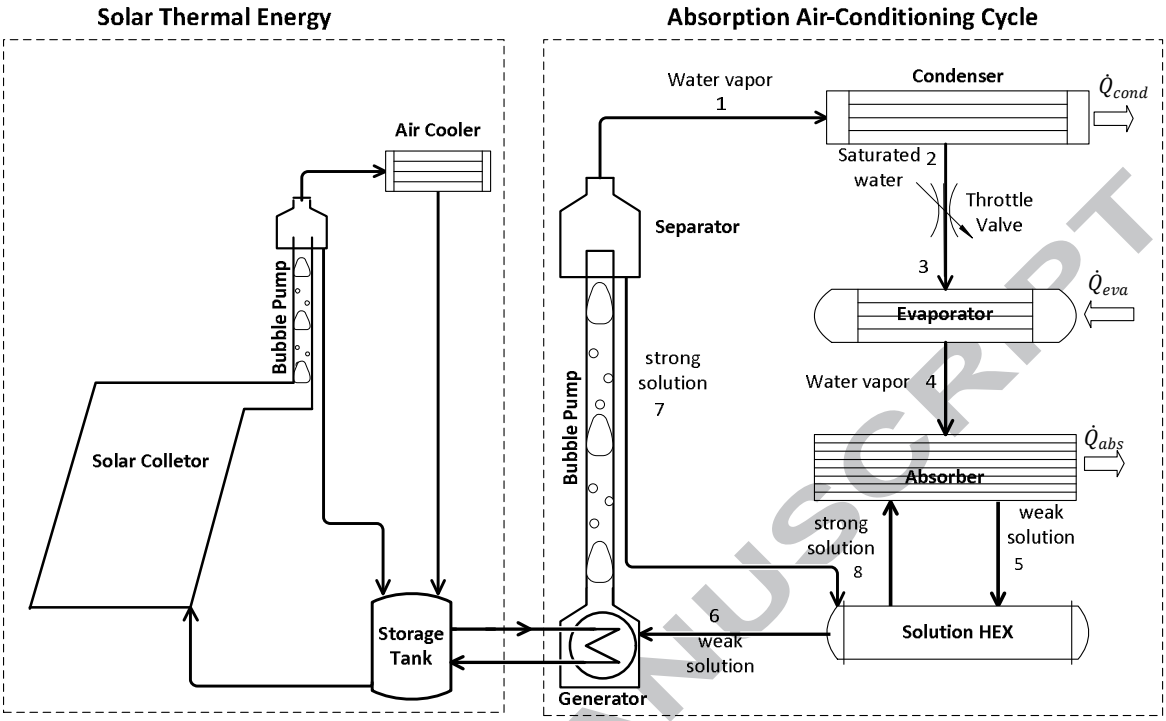

Figure 1: Flow diagram of solar absorption air-conditioning system

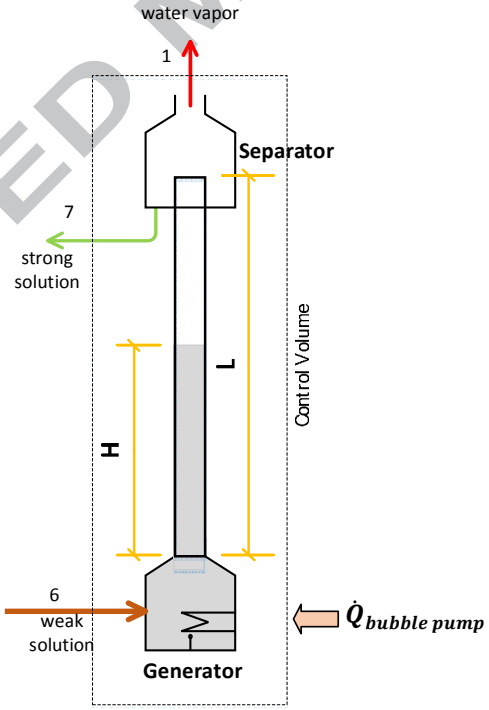

Figure 2: Bubble Pump Generator Control Volume

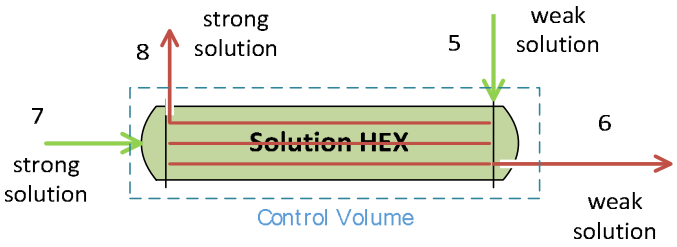

Figure 3: Solution Heat Exchanger Control Volume

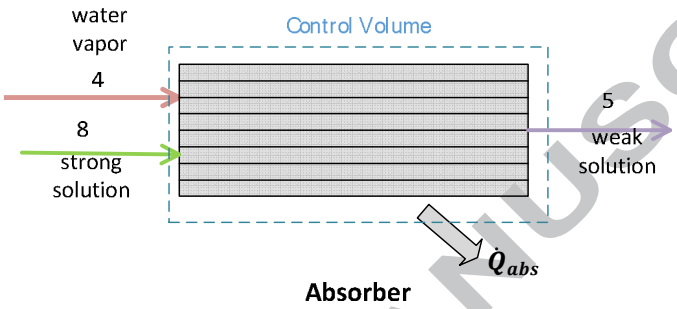

Figure 4: Absorber Control Volume

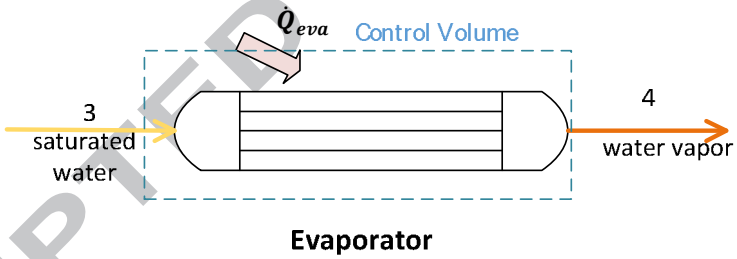

Figure 5: Evaporator Control Volume

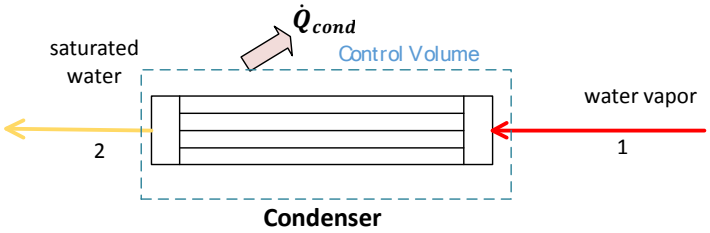

Figure 6: Condenser Control Volume

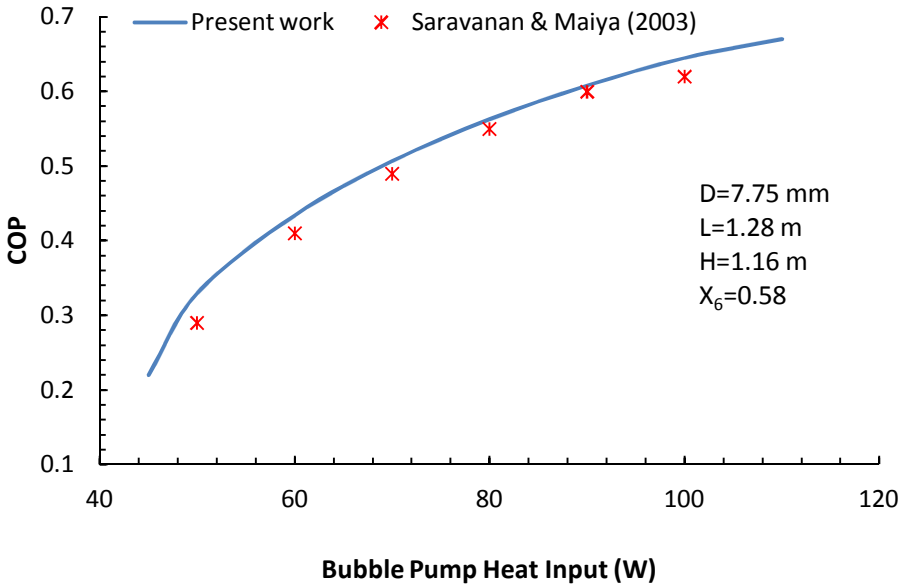

Figure 7: Performance comparison of a bubble pump operated LiBr-H_2O VARS between the proposed model and the experimental results of Saravanan & Maiya [6].

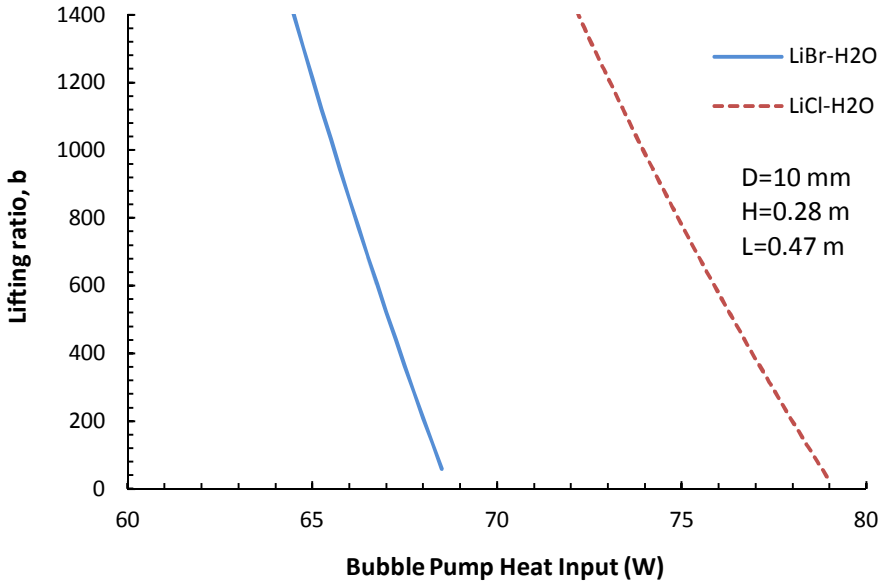

Figure 8: Lifting ratio of LiBr-H_2O and LiCl-H_2O VARS at different bubble pump heat input at T_{gen} = 70°C.

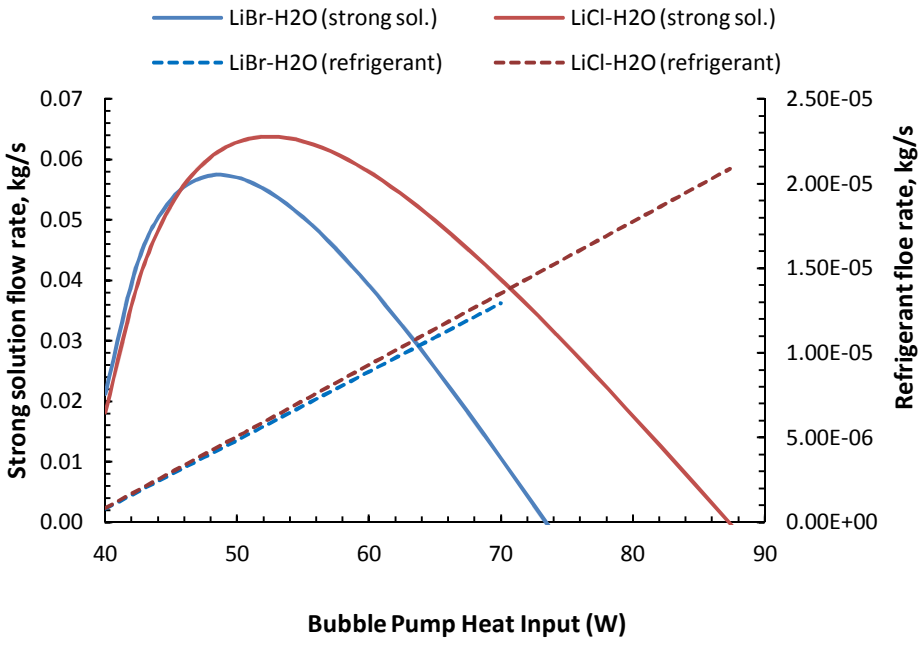

Figure 9: Strong solution and refrigerant flow rate by the bubble pump at different heat input at T_{gen} = 70°C for LiBr-H_2O and LiCl-H_2O.

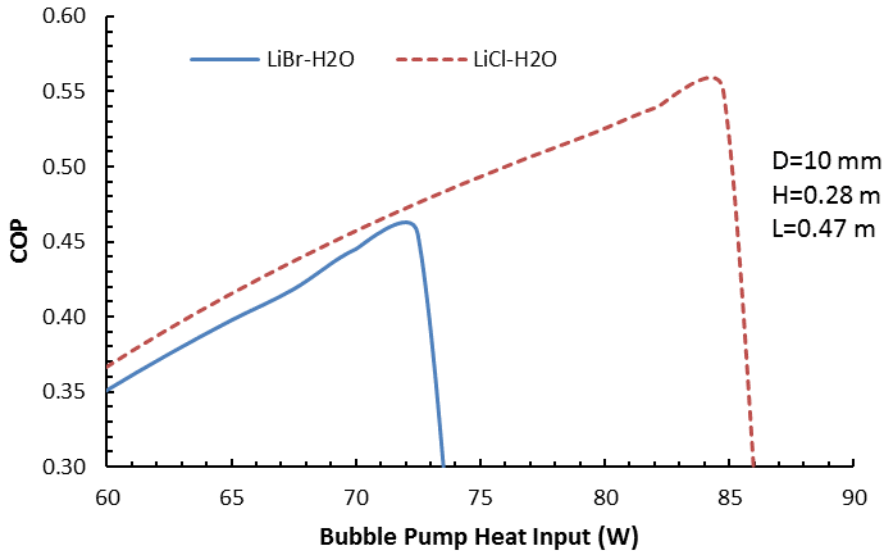

Figure 10: Coefficient of performance of LiBr-H_2O and LiCl-H_2O VARS at different bubble pump heat input at T_{gen} = 70°C, T_{cond} = 35°C, T_{abs} = 35°C, T_{eva} = 7°C, η_{HEX} = 80.

Table 1: Thermodynamic properties at different states in LiBr-H_2O and LiCl-H_2O absorption cycles at operating conditions T_{gen} = 70°C, T_{cond} = 35°C, T_{abs} = 35°C, T_{eva} = 7°C, η_{HEX} = 80, D=10 mm, H=0.28 m, and L=0.47 m.

State	Temperature (°C)	Pressure (kPa)	Mass flow (g/s)		% Concentration		Enthalpy (kJ/kg)	
			LiBr-H_2O	LiCl-H_2O	LiBr-H_2O	LiCl-H_2O	LiBr-H_2O	LiCl-H_2O
Bubble pump generator ref exit (1)	70	5.627	0.014	0.021	100	100	2630	2630
Condenser ref exit (2)	35	5.627	0.014	0.021	100	100	147	147
Evaporator ref inlet (3)	7	1.002	0.014	0.021	100	100	147	147
Evaporator ref exit (4)	7	1.002	0.014	0.021	100	100	2513	2513
Absorber sol exit (5)	35	1.002	0.672	0.413	54.08	41.07	81	155
Sol HEX exit (6)	63	1.002	0.672	0.413	54.08	41.07	139	229
Sol HEX inlet (7)	70	1.002	0.518	0.335	55.60	43.77	157	265
Absorber sol inlet (8)	44	1.002	0.518	0.335	55.60	43.77	113	186

ref = refrigerant;
sol = solution

Table 2: Thermodynamic analysis of bubble pump operated LiBr-H_2O and LiCl-H_2O absorption air-conditioning systems

	LiBr-H_2O	LiCl-H_2O
Generator Temp (°C)	70	70
Mass fract. weak sol (X_6)	54.08%	41.07%
Mass fract. strong sol (X_7)	55.6%	43.77%
Vapor Pressure (kPa)	6.5	6.8
Bubble pump, $\dot{Q}_{bubble\ pump}$	73 W	87 W
Generator, $\dot{Q}_{gen}$	73 W	87 W
Evaporator, $\dot{Q}_{eva}$	34 W	49 W
Absorber, $\dot{Q}_{abs}$	70 W	78 W
Condenser, $\dot{Q}_{cons}$	37 W	58 W
COP	0.46	0.56
Lifting ratio, b	58.85	31.48

Highlights:

- A mathematical model was developed for the operation of a bubble pump driven absorption air-conditioning system.
- A LiBr-H_2O system was modelled, and the results found to match published experimental data.
- A thermodynamic analysis of the bubble pump operated absorption system was performed.
- A new absorbent-refrigerant pair: LiCl-H_2O were used in the analysis.
- The performances of LiBr-H_2O and LiCl-H_2O systems were compared.